TECHNICAL RESEARCH REPORT

SYSTEMS RESEARCH CENTER

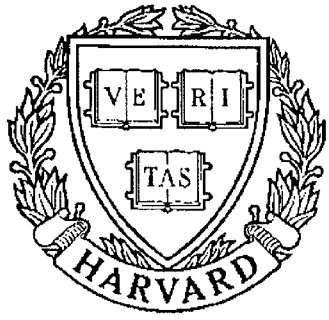

Supported by the National Science Foundation Engineering Research Center Program (NSFD CD 8803012), Industry and the University

Stabilization of Tethered Satellites During Station-Keeping

by D.-C. Liaw and E.H. Abed

TR 88-72-r1

IEEE Transactions on Automatic Control, November 1990, to appear.

Stabilization of Tethered Satellites During Station-Keeping

Der-Cherng Liaw and Eyad H. Abed

Department of Electrical Engineering
and the Systems Research Center
University of Maryland
College Park, MD 20742 USA

Abstract

After deriving a set of dynamic equations governing the dynamics of a Tethered Satellite System (TSS), stabilizing tension control laws in feedback form are derived. The tether is assumed rigid and massless, and the equations of motion are derived using the system Lagrangian. It is observed that, to stabilize the system, tools from stability analysis of critical nonlinear systems must be applied. This paper employs tools related to the Hopf Bifurcation Theorem in the construction of the stabilizing control laws, which may be taken purely linear. Simulations illustrate the nature of the conclusions, and show that nonlinear terms in the feedback can be used to significantly improve the transient response.

I. Introduction

The topic of Tethered Satellite Systems (TSS) has received considerable attention in recent years (e.g., [1]-[8], [13], [14]). Potential applications of these systems include deployment and retrieval of satellites, aiding in space-assembly tasks, use of electrodynamic tethers for electric power generation [12, p. 3-29], and tethering platforms above the Space Station for observing stellar and planetary objects [12, p. 3-85]. For other potential applications, the reader is referred to Rupp and Laue [1] and the NASA publication [12].

In this paper, we focus on the issue of stabilization of a tethered satellite system during the station-keeping mode. Specifically, consider the TSS depicted in Figure 1. Here, a large satellite is tethered to a smaller subsatellite, and the configuration is in a circular orbit around the Earth. During station-keeping, a subsatellite is controlled so as to follow a prescribed orbit to within a set tolerance [15, p. 220]. By assuming the subsatellite to be much more massive than the satellite, and that the satellite follows a perfect circular orbit, we are able to focus attention on the station-keeping control of the subsatellite. This is accomplished through the design of tether tension control laws in feedback form which result in regulating the position of the subsatellite relative to the satellite, while simultaneously regulating the tether length at a prescribed nominal value. The proposed tension control law is implemented, say, using a reel-type mechanism.

The paper makes use of several simplifying assumptions. For instance, the tether is assumed rigid and massless. With these assumptions, the TSS can be described by a set of ordinary differential equations. The system Lagrangian is used to obtain these equations. Next, we observe that linear feedback-type tension control laws can place all but two poles of the system. These two poles are a complex conjugate pair of pure imaginary eigenvalues of the system linearization. To stabilize the system, therefore, tools from stability analysis of critical nonlinear systems must be applied. Our approach is to use the technique of [10], in which Hopf bifurcation calculations are employed to construct stabilizing control laws. First, a class of purely linear stabilizing feedback control laws are given. Next, nonlinear stabilizing control laws are developed. Simulations are presented which allow one to compare the transient response of the system with the two types of feedback. The additional freedom afforded by the inclusion of nonlinear terms can be used to obtain a significant improvement in the speed of the transient response.

Notation

E - Earth

S - Satellite

m - Subsatellite and subsatellite mass

G - Gravitational constant

M, m_s - Mass of the Earth, mass of the satellite

(x_m, y_m, z_m) - Earth-based rotating Cartesian coordinates of subsatellite, with z_m in the local outgoing vertical direction, and x_m in the direction of motion of the subsatellite in its orbit (see Figure 2)

(x_s, y_s, z_s) - Earth-based rotating coordinates of the satellite

$(\hat{x}_m, \hat{y}_m, \hat{z}_m)$ - Inertial coordinates of subsatellite

$(\hat{x}_s, \hat{y}_s, \hat{z}_s)$ - Inertial coordinates of the satellite

Ω - Constant angular velocity of the satellite in circular orbit

θ, ϕ - In-plane angle and out-of-plane angle of subsatellite relative to local vertical

$\omega_\phi := \dot{\phi}$, $\omega_\theta := \dot{\theta}$, ℓ - Tether length, $v := \dot{\ell}$

r_0, r_m - Radius of the satellite orbit, radius of subsatellite orbit

τ_θ, τ_ϕ - Generalized torques in directions θ, ϕ

F_ℓ - Generalized force along tether

$\mathbf{F} := \frac{\tau_\theta}{\ell \cos\phi}\hat{\theta} + \frac{\tau_\phi}{\ell}\hat{\phi} + F_\ell \hat{\ell}$, where a hat indicates a unit vector in the given direction

$Re(\cdot) :=$ Real part of $(\cdot)$

$Im(\cdot) :=$ Imaginary part of $(\cdot)$

$i := \sqrt{-1}$

II. System Model

Referring to the depictions in Figures 1 and 2, a mathematical model of the TSS may be derived. Assume the satellite and the subsatellite are point masses and the tether is massless and rigid. Moreover, take the mass of the satellite to be much larger than that of the subsatellite (i.e., $m_s \gg m$). This allows us to take the center of mass of the TSS to be the satellite, and to consider the satellite as being in a circular orbit around the Earth. In addition, the gravitational attraction between the subsatellite and the satellite is neglected.

It is evident from Figure 2 that we have the relationships

$$x_m = \ell \cos\phi \sin\theta \tag{1}$$

$$y_m = \ell \sin\phi \tag{2}$$

$$z_m = r_0 + \ell \cos\phi \cos\theta \tag{3}$$

$$r_m^2 = r_0^2 + \ell^2 + 2r_0\ell \cos\phi \cos\theta. \tag{4}$$

Also,

$$\begin{pmatrix} \hat{x}_m \\ \hat{y}_m \\ \hat{z}_m \end{pmatrix} = \begin{pmatrix} \cos\Omega t & 0 & \sin\Omega t \\ 0 & 1 & 0 \\ -\sin\Omega t & 0 & \cos\Omega t \end{pmatrix} \begin{pmatrix} x_m \\ y_m \\ z_m \end{pmatrix}$$

$$\begin{pmatrix} \hat{x}_s \\ \hat{y}_s \\ \hat{z}_s \end{pmatrix} = \begin{pmatrix} \cos\Omega t & 0 & \sin\Omega t \\ 0 & 1 & 0 \\ -\sin\Omega t & 0 & \cos\Omega t \end{pmatrix} \begin{pmatrix} 0 \\ 0 \\ r_0 \end{pmatrix}$$

where the equations above fix a particular choice of time reference.

Since the tether is assumed to be massless, the total kinetic energy of the system is given by

$$\begin{aligned} KE &= \frac{1}{2}m_s(\dot{\hat{x}}_s^2 + \dot{\hat{y}}_s^2 + \dot{\hat{z}}_s^2) + \frac{1}{2}m(\dot{\hat{x}}_m^2 + \dot{\hat{y}}_m^2 + \dot{\hat{z}}_m^2) \\ &= \frac{1}{2}m_s\Omega^2 r_0^2 + \frac{1}{2}m\{\dot{\ell}^2 + \ell^2\dot{\phi}^2 + \ell^2\cos^2\phi(\dot{\theta}+\Omega)^2 + \Omega^2 r_0^2 \\ &\quad + 2\Omega r_0\dot{\ell}\cos\phi\sin\theta - 2\Omega r_0\ell\sin\phi\sin\theta\dot{\phi} + 2\Omega r_0\ell\cos\phi\cos\theta(\dot{\theta}+\Omega)\}. \end{aligned} \tag{5}$$

The potential energy of the system arises solely from gravity and is given by

$$PE = -\frac{GMm_s}{r_0} - \frac{GMm}{r_m}.$$

Moreover, since the satellite is assumed to be in a circular orbit, it is in a zero-g orbit. Thus

$$\frac{GMm_s}{r_0^2} = m_s\Omega^2 r_0,$$

or more succinctly $GM = \Omega^2 r_0^3$. Writing the expression for the system Lagrangian $L = KE - PE$ and invoking the Lagrangian formulation of dynamics, the dynamic equations of the system are found to be

$$\tau_\theta = m\ell^2\cos^2\phi\{\ddot{\theta} + 2\frac{\dot{\ell}}{\ell}(\dot{\theta}+\Omega) - 2\tan\phi(\dot{\theta}+\Omega)\dot{\phi}$$

$$+ \frac{\Omega^2 r_0 \sin\theta}{\ell \cos\phi}(1 - \frac{r_0^3}{r_m^3})\} \tag{6}$$

$$\tau_\phi = m\ell^2\{\ddot{\phi} + 2\frac{\dot{\ell}}{\ell}\dot{\phi} + \cos\phi\sin\phi(\dot{\theta}+\Omega)^2$$

$$+ \frac{\Omega^2 r_0}{\ell}\cos\theta\sin\phi(1 - \frac{r_0^3}{r_m^3})\} \tag{7}$$

$$F_\ell = m\{\ddot{\ell} - \ell(\dot{\phi})^2 - \ell\cos^2\phi(\dot{\theta}+\Omega)^2$$

$$+ \frac{\Omega^2 r_0^3 \ell}{r_m^3} - \Omega^2 r_0\cos\phi\cos\theta(1 - \frac{r_0^3}{r_m^3})\}. \tag{8}$$

For the limiting case $r_0 \gg \ell$, we have $r_m \simeq r_0$, and Eq. (4) implies

$$1 - \frac{r_0^3}{r_m^3} \simeq 3\cos\phi\cos\theta\frac{\ell}{r_0}. \tag{9}$$

Using Eq. (9), the approximate motion equation of the system for the case $r_0 \gg \ell$ is found to be

$$\mathbf{F} = m\hat{\ell}\{\ddot{\ell} - \ell\dot{\phi}^2 - \ell\cos^2\phi(\dot{\theta}+\Omega)^2 + \ell\Omega^2 - 3\Omega^2\ell\cos^2\phi\cos^2\theta\}$$

$$+ m\hat{\theta}\{\ddot{\theta}\ell\cos\phi + 2(\dot{\theta}+\Omega)(\dot{\ell}\cos\phi - \ell\dot{\phi}\sin\phi) + 3\ell\Omega^2\cos\theta\cos\phi\sin\theta\}$$

$$+ m\hat{\phi}\{\ell\ddot{\phi} + 2\dot{\ell}\dot{\phi} + \ell\cos\phi\sin\phi(\dot{\theta}+\Omega)^2 + 3\ell\Omega^2\cos^2\theta\cos\phi\sin\phi\},$$

which agrees with the model derived by Arnold [2] using the gravity gradient method. Note that, in the analysis of the following sections, we do not assume $r_0 \gg \ell$.

III. Analysis and Control in the Station-Keeping Mode

III.1. Model in State-Space Form

Suppose $\cos\phi \neq 0$ (i.e., $\phi \neq \pm\frac{\pi}{2}$) and let the applied tension force be the only external force acting on the system. Thus, for instance, we neglect effects of a rotating atmosphere, the Earth's magnetic force, solar radiation, and the oblateness of the Earth. We do not take into account the mechanism for commanding the desired tether tension, although one can imagine it to be controlled by a reel mechanism.

Since (i) we have modeled the satellite and subsatellite as point masses, (ii) the tether is assumed rigid, and (iii) there are no external forces besides the commanded tether

tension, we conclude that the generalized forces acting on the subsatellite are $F_\ell = T$, $\tau_\theta = 0$, $\tau_\phi = 0$. Eqs. (6)-(8) can now be rewritten in state space form as follows:

$$\dot{\phi} = \omega_\phi \tag{10}$$

$$\dot{\omega}_\phi = -\frac{2v}{\ell}\omega_\phi - \frac{1}{2}\sin(2\phi)(\omega_\theta + \Omega)^2 - \frac{\Omega^2 r_0}{\ell}\cos\theta\sin\phi(1 - \frac{r_0^3}{r_m^3}) \tag{11}$$

$$\dot{\theta} = \omega_\theta \tag{12}$$

$$\dot{\omega}_\theta = -\frac{2v}{\ell}(\omega_\theta + \Omega) + 2\tan\phi(\omega_\theta + \Omega)\omega_\phi - \frac{\Omega^2 r_0 \sin\theta}{\ell\cos\phi}(1 - \frac{r_0^3}{r_m^3}) \tag{13}$$

$$\dot{\ell} = v \tag{14}$$

$$\dot{v} = \ell\omega_\phi^2 + \ell\cos^2\phi(\omega_\theta + \Omega)^2 - \frac{\Omega^2 r_0^3 \ell}{r_m^3}$$

$$+ \Omega^2 r_0 \cos\theta\cos\phi(1 - \frac{r_0^3}{r_m^3}) + \frac{T}{m}. \tag{15}$$

For the case in which the tether length is held constant (i.e., $\dot{\ell} = v = 0$, $\ell = \ell^* =$ a constant), the conditions for an equilibrium point are $\theta = n\pi$ and $\phi = m\pi$, where n, m are integers. (We disregard another apparent possibility for ϕ, since the corresponding equation has no solution for ϕ when $\theta = n\pi$.) At the equilibrium point $(0,0,0,0)$ when only Eqs. (10)-(13) are considered with $v = 0$, the linearized system of Eqs. (10)-(13) has the two conjugate pairs of pure imaginary eigenvalues

$$\lambda_{1,2} = \pm i\Omega\sqrt{1 + \frac{r_0}{\ell^*}(1 - \frac{r_0^3}{r_{m,0}^3})}, \qquad \text{and} \tag{16}$$

$$\lambda_{3,4} = \pm i\Omega\sqrt{\frac{r_0}{\ell^*}(1 - \frac{r_0^3}{r_{m,0}^3})}, \tag{17}$$

where

$$r_{m,0} := r_0 + \ell^*. \tag{18}$$

The eigenvalues $\lambda_{1,2}$ are associated with Eqs. (10) and (11), i.e., with the out-of-plane dynamics, and $\lambda_{3,4}$ are associated with Eqs. (12) and (13), i.e., with the in-plane dynamics.

The appearance of pure imaginary eigenvalues suggests the possibility of oscillations near the equilibrium point $(0,0,0,0)$. Specifically, if the reel mechanism acts like a latch,

resulting in a fixed tether length, the system may have librations with two distinct frequencies along with the orbital motion.

In the sequel, we consider the problem of designing tension control laws rendering the TSS asymptotically stable in the station-keeping mode. The main difficulty will be the presence of the two pairs of pure imaginary eigenvalues, and the uncontrollability of one of these pairs.

The conditions for an equilibrium point of system (10)-(15) are

$$0 = \Omega^2 \sin\phi\{ \cos\phi + \frac{r_0}{\ell}\cos\theta(1 - \frac{r_0^3}{r_m^3}) \} \tag{19}$$

$$0 = \frac{\Omega^2 r_0 \sin\theta}{\ell\cos\phi}(1 - \frac{r_0^3}{r_m^3}) \tag{20}$$

$$0 = \ell\Omega^2\cos^2\phi - \frac{\Omega^2 r_0^3 \ell}{r_m^3} + \Omega^2 r_0 \cos\theta\cos\phi(1 - \frac{r_0^3}{r_m^3}) + \frac{T}{m} \tag{21}$$

where the applied tension force T (applied through a reel mechanism) may be constrained to satisfy (21). From the definition of out-of-plane angle ϕ, we have $-\frac{\pi}{2} \leq \phi \leq \frac{\pi}{2}$. There are hence only two equilibrium points: (0, 0, 0, 0, ℓ^*, 0) and (0, 0, π, 0, ℓ^*, 0) if the tether length is fixed at, say, $\ell = \ell^*$. In our paper [9], it is observed that the set $\phi = 0$, $\omega_\phi = 0$ is an invariant manifold for Eqs. (10)-(15), regardless of the form of the tension control law T. Although this implies that the system (10)-(15) is uncontrollable, we find below that there does exist a control strategy stabilizing the system. With an assumed rigid and massless tether, there may appear to be no constraint on the value of the applied tension force T. In reality, however, the tether is not rigid. Thus the subsatellite cannot be pushed away from the satellite by the applied tension force through the tether. Note that, in this paper, the sign convention implies that a positive value of tension would correspond to a slack tether. Hence, in the sequel we restrict the applied tension force T to assume only nonpositive values. Although the conclusions we will reach will also apply to the *model* (10)-(15) in the absence of this restriction, they would no longer relate to the physical problem.

III.2. Stabilization for In-Plane Angle Near $\theta = 0$

Let $x_0 = (0, 0, 0, 0, \ell^*, 0)^T$ and $X = x - x_0$, where $x = (\phi,\, \omega_\phi,\, \theta,\, \omega_\theta,\, \ell,\, v)^T$. Then the Taylor expansion of the right side of Eqs. (10)-(15) is, to third order in X,

$$\frac{d}{dt}X = L_0 X + Q_0(X,X) + C_0(X,X,X) + eU + e\frac{T}{m} \tag{22}$$

where the matrix L_0, the quadratic form Q_0, the cubic form C_0, the vector e and the scalar U are given, in terms of parameters a_i defined in Appendix A, by

$$L_0 = \begin{pmatrix} 0 & 1 & 0 & 0 & 0 & 0 \\ -a_1^2 & 0 & 0 & 0 & 0 & 0 \\ 0 & 0 & 0 & 1 & 0 & 0 \\ 0 & 0 & -a_2^2 & 0 & 0 & -\frac{2\Omega}{\ell^*} \\ 0 & 0 & 0 & 0 & 0 & 1 \\ 0 & 0 & 0 & 2\ell^*\Omega & a_3 & 0 \end{pmatrix}$$

$$Q_0(X,X) = \begin{pmatrix} 0 \\ -2\Omega\phi\omega_\theta + a_{12}\phi\tilde{\ell} - \frac{2}{\ell^*}\omega_\phi v \\ 0 \\ a_{12}\theta\tilde{\ell} - \frac{2}{\ell^*}\omega_\theta v + 2\Omega\phi\omega_\phi + \frac{2\Omega}{\ell^{*2}}\tilde{\ell}v \\ 0 \\ a_4\theta^2 + \ell^*\omega_\theta^2 + 2\Omega\omega_\theta\tilde{\ell} + a_5\phi^2 + \ell^*\omega_\phi^2 + a_{13}\tilde{\ell}^2 \end{pmatrix}$$

$$C_0(X,X,X) = \begin{pmatrix} 0 \\ a_6\theta^2\phi - \omega_\theta^2\phi + a_7\phi^3 + a_8\phi\tilde{\ell}^2 + \frac{2}{\ell^{*2}}\omega_\phi\tilde{\ell}v \\ 0 \\ a_9\theta^3 + a_{10}\theta\phi^2 + a_8\theta\tilde{\ell}^2 + 2\phi\omega_\phi\omega_\theta + \frac{2}{\ell^{*2}}\omega_\theta\tilde{\ell}v - \frac{2\Omega}{\ell^{*3}}\tilde{\ell}^2 v \\ 0 \\ a_{14}\theta^2\tilde{\ell} + \omega_\theta^2\tilde{\ell} - 2\ell^*\Omega\omega_\theta\phi^2 + a_{11}\phi^2\tilde{\ell} + \omega_\phi^2\tilde{\ell} + a_{15}\tilde{\ell}^3 \end{pmatrix}$$

$$e = (0, 0, 0, 0, 0, 1)^T$$

$$U = \frac{(3r_0^2\ell^* + 3r_0\ell^{*2} + \ell^{*3})\Omega^2}{(r_0 + \ell^*)^2}$$

where $\tilde{\ell} := \ell - \ell^*$. The expressions above have been verified using the code MACSYMA.[1]

Case 1: Linear State Feedback

[1] MACSYMA is a trademark of Symbolics, Inc., Cambridge, MA.

Our first design is that of a tension control law in linear state feedback form which stabilizes the system. The design is carried out in two steps. The first, addressed in Lemma 1 and Corollary 1 below, is to give conditions on the linear state feedback ensuring that four of the eigenvalues of system (10)-(15) are moved to the left half of the complex plane. These eigenvalues correspond to the "in-plane variables" $(\theta,\ \omega_\theta,\ \tilde{\ell},\ v)$.

Lemma 1. If the following conditions hold, then the tension control force $T = m(-U - k_1\theta - k_2\omega_\theta - k_3\tilde{\ell} - k_4 v)$ stabilizes the "in-plane Jacobian matrix" at the equilibrium point x_0, i.e., the Jacobian matrix of Eqs. (12)-(15) with respect to the vector $(\theta, \omega_\theta, \tilde{\ell}, v)$:

(i) $k_4 > 0$

(ii) $b_1, b_2, b_3 > 0$

(iii) $k_4 b_1 b_2 - b_2^2 - k_4^2 b_3 > 0$

where

$$b_1 = k_3 - \frac{(2r_0\ell^{*2} + \ell^{*3})\Omega^2}{(r_0 + \ell^*)^3} - \frac{2\Omega k_2}{\ell^*} + 4\Omega^2, \tag{23}$$

$$b_2 = \frac{k_4(3r_0^3 + 3r_0^2\ell^* + r_0\ell^{*2})\Omega^2}{(r_0 + \ell^*)^3} - \frac{2\Omega k_1}{\ell^*}, \tag{24}$$

$$b_3 = \frac{(3r_0^3 + 3r_0^2\ell^* + r_0\ell^{*2})\Omega^2}{(r_0 + \ell^*)^3}(k_3 - \frac{(3r_0^3 + 3r_0^2\ell^* + 3r_0\ell^{*2} + \ell^{*3})\Omega^2}{(r_0 + \ell^*)^3}). \tag{25}$$

Sketch of proof: The linearization of (22) upon application of the linear state feedback T above is given by

$$\frac{d}{dt}X = \tilde{L}_0 X$$

where

$$\tilde{L}_0 = \begin{pmatrix} 0 & 1 & 0 & 0 & 0 & 0 \\ -a_1^2 & 0 & 0 & 0 & 0 & 0 \\ 0 & 0 & 0 & 1 & 0 & 0 \\ 0 & 0 & -a_2^2 & 0 & 0 & -\frac{2\Omega}{\ell^*} \\ 0 & 0 & 0 & 0 & 0 & 1 \\ 0 & 0 & -k_1 & -k_2 + 2\ell^*\Omega & -k_3 + a_3 & -k_4 \end{pmatrix}$$

Hence the characteristic equation of the closed-loop system is

$$(\lambda^2 + a_1^2)\ (\lambda^4 + k_4\lambda^3 + b_1\lambda^2 + b_2\lambda + b_3) = 0 \tag{26}$$

where b_i, $i = 1, \ldots, 3$ are as defined in Eqs. (23)-(25). The lemma follows readily by applying the Routh-Hurwitz test to the second polynomial factor in the left side of Eq. (26).

The next result follows readily from Lemma 1, and demonstrates that the set of feedbacks of Lemma 1 is not vacuous, at least in the practically interesting case $r_0 \gg \ell^*$. The result also holds for larger ℓ^*, but the corresponding conditions on the feedback gains become very complicated.

Corollary 1. If $r_0 \gg \ell^*$, the conclusion of Lemma 1 holds when any of the following three conditions is satisfied:

(i) $0 \geq k_1 > \ell^* \Omega k_4 (1 - \frac{k_3}{2\Omega^2})$, $k_2 = 0$, $k_3 > 3\Omega^2$, and $k_4 > 0$;

(ii) $0 > k_1 > k_2 k_4$, $k_2 < 0$, $k_3 > 3\Omega^2$, and $k_4 > 0$;

(iii) $k_1 = 0$, $k_2 < \min\{2\Omega\ell^*, \frac{\ell^*}{2\Omega} k_3 + 3\Omega^2\}$, $k_3 > 3\Omega^2$, and $k_4 > 0$.

From the closed-loop characteristic equation (26), we infer that the system has an uncontrollable pair of pure imaginary eigenvalues. Moreover, it is easy to see that even when the states ϕ and ω_ϕ are used in the tension control law, these two pure imaginary eigenvalues remain fixed. Hence the stability of the closed-loop system cannot be identified from the linearized model alone.

The closed-loop system (upon application of a feedback law as in Lemma 1 or Corollary 1) is approximated, to third order in X, by

$$\frac{d}{dt} X = \tilde{L}_0 X + Q_0(X, X) + C_0(X, X, X) \tag{27}$$

in which $\tilde{L}_0$ has a complex conjugate pair of pure imaginary eigenvalues, with the remaining eigenvalues in the left half of the complex plane. This situation is an example of a *critical case* in nonlinear stability analysis. Its resolution may be approached via results on Hopf bifurcation for one-parameter families of nonlinear systems (see, e.g., [16]). The local asymptotic stability of the origin of Eq. (27) can be concluded from the negativity of an associated "stability coefficient," often denoted by β_2. The value of this coefficient can be obtained in several ways. One can, for instance, study normal forms of Eq. (27). Alternatively, one observes that, in the situation at-hand, smooth parametrizations of (27) will typically exhibit a Hopf bifurcation. The stability of the bifurcated periodic solutions, as well as that of the origin of (27), follows from the negativity of the Floquet

exponents of these periodic solutions. The stability coefficient β_2 can be obtained as the leading coefficient in an asymptotic expansion of the critical Floquet exponent. The coefficient β_2 may be computed systematically. When $\beta_2 < 0$, the equilibrium point is locally asymptotically stable, while $\beta_2 > 0$ implies instability of the equilibrium. The case $\beta_2 = 0$ is inconclusive regarding stability. We now proceed to use an algorithm for the computation of β_2 (see for instance [10], [16]) to determine the dependence of β_2 on the gains k_i, $i = 1, \ldots, 4$.

Denote by r and l the right (column) and left (row) eigenvectors, respectively, of $\tilde{L}_0$ corresponding to the imaginary eigenvalue ia_1. Requiring $lr = 1$, we have

$$r = (1, ia_1, 0, 0, 0, 0)^T \tag{28}$$

$$l = (\frac{1}{2}, -i\frac{1}{2a_1}, 0, 0, 0, 0) \tag{29}$$

Next, solve the equations

$$-\tilde{L}_0 a = \frac{1}{2} Q_0(r, \bar{r}), \tag{30}$$

$$(2ia_1 I - \tilde{L}_0) b = \frac{1}{2} Q_0(r, r) \tag{31}$$

for the vectors a and b. Here, an overbar denotes complex conjugation and I denotes the identity matrix. We find

$$a = (0, 0, 0, 0, -\frac{a_5 - \ell^* a_1^2}{2(a_3 - k_3)}, 0)^T \tag{32}$$

$$b = (0, 0, c_1, c_2, c_3, c_4)^T \tag{33}$$

where the a_i are as in Appendix A, and the c_i and d_i are given by

$$c_1 = \frac{1}{d_1 + id_2} \{ \frac{a_5}{2} + \frac{\ell^* a_1^2}{2} - \frac{\ell^*}{4}(k_3 - a_3) - \frac{i}{2} k_4 a_1 \ell^* \} \tag{34}$$

$$c_2 = 2ia_1 c_1 \tag{35}$$

$$c_3 = \frac{\ell^*}{4} - \frac{i\ell^*(4a_1^2 - a_2^2)}{4a_1 \Omega} c_1 \tag{36}$$

$$c_4 = \frac{i\ell^* a_1}{2} + \frac{\ell^*(4a_1^2 - a_2^2)}{2\Omega} c_1 \tag{37}$$

and

$$d_1 = k_1 + \frac{\ell^* k_4}{2\Omega}(4a_1^2 - a_2^2) \tag{38}$$

$$d_2 = 2a_1(k_2 - 2\ell^*\Omega) + \frac{\ell^*(4a_1^2 - a_2^2)}{4a_1\Omega}(a_3 + 4a_1^2 - k_3) \tag{39}$$

In general, the value of the bifurcation stability coefficient β_2 is given by the formula

$$\beta_2 = 2Re\{2lQ_0(r,a) + lQ_0(\bar{r},b) + \frac{3}{4}lC_0(r,r,\bar{r})\} \tag{40}$$

In our case, we then have

$$\begin{aligned}\beta_2 &= \frac{1}{a_1}\{-\Omega Im(c_2) + \frac{(6r_0^3 + 4r_0^2\ell^* + r_0\ell^{*2})\Omega^2}{2(r_0+\ell^*)^4}Im(c_3) + \frac{a_1}{\ell^*}Re(c_4)\} \\ &= \frac{d_3}{a_1}\cdot Re(c_1)\end{aligned} \tag{41}$$

where (assuming $\ell^* < r_0$)

$$d_3 = -2a_1\Omega - \frac{\ell^*(4a_1^2 - a_2^2)}{8a_1\Omega}\frac{(6r_0^3 + 4r_0^2\ell^* + r_0\ell^{*2})\Omega^2}{(r_0+\ell^*)^4} + \frac{a_1(4a_1^2 - a_2^2)}{2\Omega} > 0 \tag{42}$$

$$Re(c_1) = \frac{1}{d_1^2 + d_2^2}\{(\frac{a_5}{2} + \frac{\ell^* a_1^2}{2} - \frac{\ell^*}{4}(k_3 - a_3))d_1 - \frac{1}{2}k_4 a_1 \ell^* d_2\} \tag{43}$$

Since $a_1 > 0$, $d_3 > 0$, and since stability is implied by $\beta_2 < 0$, we have the following result.

Theorem 1. If a linear state feedback controller T as defined in Lemma 1 is applied, with

$$(\frac{a_5}{2} + \frac{\ell^* a_1^2}{2} - \frac{\ell^*}{4}(k_3 - a_3))d_1 - \frac{1}{2}k_4 a_1 \ell^* d_2 < 0,$$

then the equilibrium point x_0 will be rendered asymptotically stable for the system (10)-(15).

The next result readily follows from Theorem 1 and Corollary 1.

Corollary 2. If $r_0 \gg \ell^*$ and a linear state feedback control T as in Lemma 1 is applied, with either of the following three conditions satisfied, then the conclusion of Theorem 1 holds:

(i) $0 \geq k_1 > \ell^*\Omega k_4(1 - \frac{k_3}{2\Omega^2})$, $k_2 = 0$, $3\Omega^2 < k_3 < 14\Omega^2$, and $k_4 > 0$;

(ii) $0 > k_1 > k_2 k_4$, $0 > k_2 > 2\ell^*\Omega - \frac{13\ell^*\Omega}{32}(19 - \frac{k_3}{\Omega^2})$, $3\Omega^2 < k_3 < 14\Omega^2$, and $k_4 > 0$;

(iii) $k_1 = 0$, $\min\{2\Omega\ell^*, 3\Omega^2\} > k_2 > 2\ell^*\Omega - \frac{13\ell^*\Omega}{32}(19 - \frac{k_3}{\Omega^2})$, $3\Omega^2 < k_3 < 14\Omega^2$, and $k_4 > 0$.

Case 2: Nonlinear State Feedback

Next we present a result on stabilization with a tension control law including both linear and nonlinear terms. The nonlinear terms introduce more flexibility in the design, and, as will be seen in Section IV, can lead to superior transient response.

By computing the eigenvectors l and r and using the formula (40) for β_2, we find that *any cubic term in the feedback has no effect on the value of* β_2. We are therefore led to hypothesize a *feedback containing only linear and quadratic terms.* The component of the closed-loop quadratic term $Q_0(X, X)$ depending on the states θ, ω_θ, $\tilde{\ell}$ or v is also found to have no effect on β_2. The next theorem gives conditions for a nonlinear feedback, of the form motivated by these observations, to be stabilizing.

Theorem 2. If condition (44) below holds, then the applied tension control force $T = m(-U - k_1\theta - k_2\omega_\theta - k_3\tilde{\ell} - k_4 v - q_1\phi^2 - q_2\phi\omega_\phi - q_3\omega_\phi^2)$ stabilizes the system (10)-(15), where the k_i, $i = 1, \ldots, 4$ satisfy the conditions of Lemma 1.

$$(\frac{-q_1 + a_5}{2} + (\frac{\ell^* + q_3}{2})a_1^2 - (k_3 - a_3)\frac{\ell^*}{4})d_1 + \frac{a_1}{2}(-q_2 - \ell^* k_4)d_2 < 0 \qquad (44)$$

Here, d_1, d_2 are given in Eqs. (38) and (39), and the a_i are as specified in Appendix A.

The proof entails checking the effect on the value of β_2 of adding the extra quadratic term $-(q_1\phi^2 + q_2\phi\omega_\phi + q_3\omega_\phi^2)$ in the last row of $Q_0(X, X)$.

As mentioned above, inclusion of nonlinear terms in the feedback control may be used to improve the transient response of the stabilized system. In particular, the rate at which system trajectories decay toward the equilibrium point may be significantly increased. Simulation evidence for this is given in Section IV.

It is not difficult to give analytical reasoning to support this conclusion, and to guide in the tuning of the linear and quadratic feedback gains. Assume $r_0 \gg \ell^*$, and use Eq. (40) with a feedback of the form given in Theorem 2 to ascertain the approximate formula

$$\beta_2 \simeq \frac{9\Omega}{2(d_1^2 + d_2^2)}\{(\frac{-q_1 + a_5}{2} + (\frac{\ell^* + q_3}{2})a_1^2 - (k_3 - a_3)\frac{\ell^*}{4})d_1$$

$$+ \frac{a_1}{2}(-q_2 - \ell^* k_4)d_2\} \tag{45}$$

Eq. (45) can be used to show that, if $r_0 \gg \ell^*$ and the linear gains k_i, $i = 1, \ldots, 4$, are chosen according to condition (i) of Corollary 2, with $k_1 = 0$, then β_2 may be rendered as negative as desired simply by setting the quadratic gains $q_2 = q_3 = 0$ and taking $q_1 > 0$ and sufficiently large. Thus the gains k_i may be used to place four of the eigenvalues of (10)-(15) in the left half of the complex plane, while, *independently*, the gains q_i, $i = 1,2,3$, are used to make β_2 negative and of large magnitude.

III.3. Stabilization for In-Plane Angle Near $\theta = \pi$

Similarly, now let $x_\pi = (0, 0, \pi, 0, \ell^*, 0)^T$ denote the equilibrium point of interest, and $X = x - x_\pi$ be the differential state variation. Then the system (10)-(15), to third order near the equilibrium point x_π, may be written as follows

$$\frac{d}{dt}X = L_\pi X + Q_\pi(X, X) + C_\pi(X, X, X) + eU_\pi + e\frac{T}{m}$$

Here, L_π, Q_π, C_π are as identified in Appendix B. The next lemma is analogous to Lemma 1, and so is stated without proof.

Lemma 2. Let the applied tension force be of the form $T = m(-U_\pi - k_1\tilde{\theta} - k_2\omega_\theta - k_3\tilde{\ell} - k_4 v)$, where $\tilde{\theta} := \theta - \pi$ and $\omega_\theta := \dot{\tilde{\theta}} = \dot{\theta}$. Then the "in-plane" Jacobian matrix of Eqs. (12)-(15), i.e., the Jacobian of the right side of (12)-(15) with respect to $(\tilde{\theta}, \omega_\theta, \tilde{\ell}, v)$, will be stable at the equilibrium point x_π, if k_i, $i = 1, \ldots, 4$, satisfy the following conditions:

(i) $k_4 > 0$,

(ii) $h_1, h_2, h_3 > 0$, and

(iii) $k_4 h_1 h_2 - h_2^2 - k_4^2 h_3 > 0$.

Here, the auxiliary parameters h_1, h_2, h_3 are given by

$$h_1 = k_3 - \frac{(2r_0\ell^{*2} - \ell^{*3})\Omega^2}{(r_0 - \ell^*)^3} - \frac{2\Omega k_2}{\ell^*} + 4\Omega^2, \tag{46}$$

$$h_2 = \frac{k_4(3r_0^3 - 3r_0^2\ell^* + r_0\ell^{*2})\Omega^2}{(r_0 - \ell^*)^3} - \frac{2\Omega k_1}{\ell^*}, \tag{47}$$

$$h_3 = \frac{(3r_0^3 - 3r_0^2\ell^* + r_0\ell^{*2})\Omega^2}{(r_0 - \ell^*)^3}(k_3 - \frac{(3r_0^3 - 3r_0^2\ell^* + 3r_0\ell^{*2} - \ell^{*3})\Omega^2}{(r_0 - \ell^*)^3}). \tag{48}$$

Corollaries 1 and 2 remain valid. The detailed statements need not be given.

IV. Simulation Results

A TSS with the following characteristics is considered:

- Nominal tether length $\ell^* = 100$ km,
- Orbital radius $r_0 = 6598$ km,
- Subsatellite mass $m = 170$ kg,
- Orbital angular velocity $\Omega = 0.0011781$ radians/second.

Let the equilibrium point of interest of (10)-(15) be $x_0 = (0, 0, 0, 0, \ell^*, 0)$. Simulation results will now be presented which illustrate the system dynamics for the various types of control studied in this paper.

Let the initial conditions of the system be $\phi = 0.01$ radians, $\theta = -0.01$ radians, and $\omega_\theta = \omega_\phi = 0$.

Example IV.1. (No tension control: latch mechanism)

Suppose the reel mechanism acts like a latch fixing ℓ at ℓ^*. The system response for the in-plane angle θ and the out-of-plane angle ϕ is shown in Figures 3(a) and 3(b), respectively. We observe an apparent undamped oscillation near the equilibrium point x_0.

Example IV.2. (Linear stabilizing feedback)

The tension controller is taken as $T = -m(U + k_3\tilde{\ell} + k_4 v)$, with $k_3 = 3.1\Omega^2$, $k_4 = 0.0034$, and $U = 0.41019$. The control law is stabilizing, as can be checked using Theorem 1. Indeed, $\beta_2 \simeq -0.0004$ for the closed-loop system. The response of the variables of ϕ, θ, and the deviation $\tilde{\ell}$ of the tether length are shown in Figures 4(a), 4(b) and 4(c), respectively. However, it is not easy to see in Figure 4(a) any decay of the oscillation in the out-of-plane angle ϕ. This may be attributed to the fact that $|\beta_2|$ is small. The applied tension force is shown in Figure 4(d).

Example IV.3. (Linear-plus-quadratic stabilizing feedback)

Let the tension control law be of the form

$$T = -m(U + k_3\tilde{\ell} + k_4 v + q_1\phi^2 + q_2\phi\omega_\phi + q_3\omega_\phi^2), \tag{49}$$

where $U = 0.41019$. The out-of-plane angle ϕ decays when $k_3 = 3.1\Omega^2$, $k_4 = 0.0034$, $q_1 = 1500$, and $q_2 = q_3 = 0$ as, shown in Figure 5(a). However, this is at the expense of large variations in θ and $\tilde{\ell}$, as depicted in Figures 5(b) and 5(c). The applied tension force is shown in Figure 5(d).

Example IV.4. (Linear-plus-quadratic stabilizing feedback)

A further example is depicted in Figure 6. In this example, k_3, k_4 and q_3 are unchanged from their previous values (given in Example IV.3), but now $q_1 = 0$, and $q_2 = 10^6$.

Example IV.5. (Switching-type stabilizing feedback)

Figure 7 relates to an example invoking a switching control strategy. The nonlinear feedback control law of Example IV.3 is used for the first 5 hours of the simulation. Then the control law is switched to a purely linear feedback with the parameters values specified in Example IV.2.

V. Concluding Remarks

In this paper, we have presented analytical designs of tension feedback control laws for the stabilization of the tethered satellite system during station-keeping. These designs are based on calculations related to Hopf bifurcation stability. The calculations have been performed for a model of the tethered satellite system derived under several simplifying assumptions. This model is characterized by its nonlinearity and the existence of two critical modes, one of which cannot be removed by (linear) feedback. Notwithstanding this fact, we have been able to construct stabilizing controllers using linear and/or quadratic feedback. Cubic terms were not included in the feedback laws since the nonlinear stability calculations indicated that their effect might be of only secondary significance. Moreover, simulation was used to demonstrate the validity of the analytical designs. The simulations also indicated the importance of quadratic feedback of the out-of-plane angle ϕ and/or the out-of-plane angular rate ω_ϕ in improving the transient response of the out-of-plane variables, i.e., in dampening the roll oscillations.

Regarding the issue of how to achieve further improvements in the transient response, several possibilities arise. Optimization-based computer-aided design tools can be applied to systematically search for linear and/or nonlinear control gains resulting in a suboptimal transient response. If other actuators, such as subsatellite thrusters or tether base

movement, are available in addition to tether tension control, then one expects improved transient performance.

Acknowledgment

The authors are grateful to Professors P.S. Krishnaprasad and J.H. Maddocks for helpful discussions, and to the reviewers for their comments and suggestions. This research was supported in part by the Air Force Office of Scientific Research under URI Grant AFOSR-87-0073, by the National Science Foundation's Engineering Research Centers Program: NSFD CDR-88-03012, by NSF Grant ECS-86-57561, and by the TRW Foundation.

References

[1] C.C. Rupp and J.H. Laue, "Shuttle/tethered satellite system," *The Journal of the Astronautical Sciences*, Vol. 26, pp. 1-17, 1978.

[2] D.A. Arnold, "The behavior of long tethers in space," *The Journal of the Astronautical Sciences*, Vol. 35, pp. 3-18, 1987.

[3] J.B. Eades, Jr. and H. Wolf, *Tethered Body Problems and Relative Motion Orbit Determination*, Final Report, Contract NAS5-21453, Analytical Mechanics Associates, Inc., August 1972.

[4] T.R. Kane and A.K. Banerjee, "Tether deployment dynamics," *The Journal of the Astronautical Sciences*, Vol. 30, pp. 347-365, 1982.

[5] C.C. Rupp, *A Tether Tension Control Law for Tethered Subsatellites Deployed Along Local Vertical*, NASA TM X-64963, 1975.

[6] A.K. Misra and V.J. Modi, "Deployment and retrieval of shuttle supported tethered satellites," *J. Guidance*, Vol. 5, pp. 278-285, 1980.

[7] P.M. Bainum, S. Woodard and J. Juang, "The development of optimal control laws for orbiting tethered platform systems," *The Journal of the Astronautical Sciences*, Vol. 35, pp. 135-153, 1987.

[8] W.P. Baker, J.A. Dunkin, Z.J. Galaboff, K.D. Johnston, R.R. Kissel, M.H. Rheinfurth and P.L. Siebel, *Tethered Subsatellite Study*, NASA TM X-73314, 1976.

[9] E.H. Abed and D.-C. Liaw, "On the stabilization of tethered satellite systems," *Abstracts of the Second Conf. on Non-Linear Vibrations, Stability, and Dynamics of Structures and Mechanisms*, VPI, Blacksburg, VA, June 1-3, 1988.

[10] E.H. Abed and J.-H. Fu, "Local feedback stabilization and bifurcation control, I. Hopf bifurcation," *Systems and Control Letters*, Vol. 7, pp. 11-17, 1986.

[11] D.-C. Liaw and E.H. Abed, "Stability analysis and control of tethered satellites," *Model Determination for Large Space Systems Workshop*, Rept. JPL D-5574, Jet Propulsion Laboratory, Pasadena, CA, pp. 308-330, March 1988.

[12] General Research Corporation, *Tethers in Space Handbook*, 1986.

[13] V.J. Modi, C.-F. Geng, A.K. Misra and D.M. Xu, "On the control of the space shuttle based tethered systems," *Acta Astronautica*, Vol. 9, pp. 437-443, 1982.

[14] V.J. Modi, C.-F. Geng and A.K. Misra, "Effect of damping on the control dynamics of the space shuttle based tethered systems," *The Journal of the Astronautical Sciences*, Vol. 31, pp. 135-149, 1983.

[15] G. Maral and M. Bousquet, *Satellite Communications Systems.* Chichister, U.K.: Wiley, 1986.

[16] L.N. Howard, "Nonlinear oscillations," pp. 1-67 in: F.C. Hoppensteadt, Ed., *Nonlinear Oscillations in Biology.* Providence: Amer. Math. Soc., 1979.

Appendix A

The values of the coefficients a_i, $i = 1, \ldots, 15$ are as listed below.

$$a_1 = \left(\frac{(4r_0^3 + 6r_0^2\ell^* + 4r_0\ell^{*2} + \ell^{*3})}{(r_0 + \ell^*)^3}\right)^{1/2}\Omega$$

$$a_2 = \left(\frac{(3r_0^3 + 3r_0^2\ell^* + r_0\ell^{*2})}{(r_0 + \ell^*)^3}\right)^{1/2}\Omega$$

$$a_3 = \frac{(3r_0^3 + 3r_0^2\ell^* + 3r_0\ell^{*2} + \ell^{*3})\Omega^2}{(r_0 + \ell^*)^3}$$

$$a_4 = -\frac{(6r_0^4\ell^* + 6r_0^3\ell^{*2} + 4r_0^2\ell^{*3} + r_0\ell^{*4})\Omega^2}{2(r_0 + \ell^*)^4}$$

$$a_5 = -\frac{(8r_0^4\ell^* + 14r_0^3\ell^{*2} + 16r_0^2\ell^{*3} + 9r_0\ell^{*4} + 2\ell^{*5})\Omega^2}{2(r_0 + \ell^*)^4}$$

$$a_6 = \frac{(6r_0^5 + 9r_0^4\ell^* + 10r_0^3\ell^{*2} + 5r_0^2\ell^{*3} + r_0\ell^{*4})\Omega^2}{2(r_0+\ell^*)^5}$$

$$a_7 = \frac{(16r_0^5 + 29r_0^4\ell^* + 50r_0^3\ell^{*2} + 45r_0^2\ell^{*3} + 21r_0\ell^{*4} + 4\ell^{*5})\Omega^2}{6(r_0+\ell^*)^5}$$

$$a_8 = -\frac{(10r_0^3 + 5r_0^2\ell^* + r_0\ell^{*2})\Omega^2}{(r_0+\ell^*)^5}$$

$$a_9 = \frac{(12r_0^5 + 9r_0^4\ell^* + 10r_0^3\ell^{*2} + 5r_0^2\ell^{*3} + r_0\ell^{*4})\Omega^2}{6(r_0+\ell^*)^5}$$

$$a_{10} = -\frac{(27r_0^4\ell^* + 30r_0^3\ell^{*2} + 15r_0^2\ell^{*3} + 3r_0\ell^{*4})\Omega^2}{6(r_0+\ell^*)^5}$$

$$a_{11} = -\frac{(4r_0^5 + 2r_0^4\ell^* + 10r_0^3\ell^{*2} + 10r_0^2\ell^{*3} + 5r_0\ell^{*4} + \ell^{*5})\Omega^2}{(r_0+\ell^*)^5}$$

$$a_{12} = \frac{(6r_0^3 + 4r_0^2\ell^* + r_0\ell^{*2})\Omega^2}{(r_0+\ell^*)^4}$$

$$a_{13} = -\frac{3r_0^3\Omega^2}{(r_0+\ell^*)^4}$$

$$a_{14} = -\frac{(3r_0^5 - 3r_0^4\ell^*)\Omega^2}{(r_0+\ell^*)^5}$$

$$a_{15} = \frac{4r_0^3\Omega^2}{(r_0+\ell^*)^5}.$$

Appendix B

The system model (10)-(15) is approximated, to third order in the states, near the equilibrium point x_π by

$$\dot{X} = L_\pi X + Q_\pi(X,X) + C_\pi(X,X,X) + eU_\pi + e\frac{T}{m}$$

where

$$L_\pi = \begin{pmatrix} 0 & 1 & 0 & 0 & 0 & 0 \\ -f_1^2 & 0 & 0 & 0 & 0 & 0 \\ 0 & 0 & 0 & 1 & 0 & 0 \\ 0 & 0 & -f_2^2 & 0 & 0 & -\frac{2\Omega}{\ell^*} \\ 0 & 0 & 0 & 0 & 0 & 1 \\ 0 & 0 & 0 & 2\ell^*\Omega & f_3 & 0 \end{pmatrix}$$

$$Q_\pi = \begin{pmatrix} 0 \\ -2\Omega\phi\omega_\theta + f_{12}\phi\tilde{\ell} - \frac{2}{\ell^*}\omega_\phi v \\ 0 \\ f_{12}\tilde{\theta}\tilde{\ell} - \frac{2}{\ell^*}\omega_\theta v + 2\Omega\phi\omega_\phi + \frac{2\Omega}{\ell^{*2}}\tilde{\ell}v \\ 0 \\ f_4\tilde{\theta}^2 + \ell^*\omega_\theta^2 + 2\Omega\omega_\theta\tilde{\ell} + f_5\phi^2 + \ell^*\omega_\phi^2 + f_{13}\tilde{\ell}^2 \end{pmatrix}$$

$$C_\pi = \begin{pmatrix} 0 \\ f_6\tilde{\theta}^2\phi - \omega_\theta^2\phi + f_7\phi^3 + f_8\phi\tilde{\ell}^2 + \frac{2}{\ell^{*2}}\omega_\phi\tilde{\ell}v \\ 0 \\ f_9\tilde{\theta}^3 + f_{10}\tilde{\theta}\phi^2 + f_8\tilde{\theta}\tilde{\ell}^2 + 2\phi\omega_\phi\omega_\theta + \frac{2}{\ell^{*2}}\omega_\theta\tilde{\ell}v - \frac{2\Omega}{\ell^{*3}}\tilde{\ell}^2 v \\ 0 \\ f_{14}\tilde{\theta}^2\tilde{\ell} + \omega_\theta^2\tilde{\ell} - 2\ell^*\Omega\omega_\theta\phi^2 + f_{11}\phi^2\tilde{\ell} + \omega_\phi^2\tilde{\ell} + f_{15}\tilde{\ell}^3 \end{pmatrix}$$

$$e = (0,0,0,0,0,1)'$$

$$U_\pi = \frac{(3r_0^2\ell^* - 3r_0\ell^{*2} + \ell^{*3})\Omega^2}{(r_0 - \ell^*)^2}$$

and the values of f_i, $i = 1, \ldots, 15$ are

$$f_1 = (\frac{(4r_0^3 - 6r_0^2\ell^* + 4r_0\ell^{*2} - \ell^{*3})}{(r_0 - \ell^*)^3})^{1/2}\Omega$$

$$f_2 = (\frac{(3r_0^3 - 3r_0^2\ell^* + r_0\ell^{*2})}{(r_0 - \ell^*)^3})^{1/2}\Omega$$

$$f_3 = \frac{(3r_0^3 - 3r_0^2\ell^* + 3r_0\ell^{*2} - \ell^{*3})\Omega^2}{(r_0 - \ell^*)^3}$$

$$f_4 = -\frac{(6r_0^4\ell^* - 6r_0^3\ell^{*2} + 4r_0^2\ell^{*3} - r_0\ell^{*4})\Omega^2}{2(r_0 - \ell^*)^4}$$

$$f_5 = -\frac{(8r_0^4\ell^* - 14r_0^3\ell^{*2} + 16r_0^2\ell^{*3} - 9r_0\ell^{*4} + 2\ell^{*5})\Omega^2}{2(r_0 - \ell^*)^4}$$

$$f_6 = \frac{(6r_0^5 - 9r_0^4\ell^* + 10r_0^3\ell^{*2} - 5r_0^2\ell^{*3} + r_0\ell^{*4})\Omega^2}{2(r_0 - \ell^*)^5}$$

$$f_7 = \frac{(16r_0^5 - 29r_0^4\ell^* + 50r_0^3\ell^{*2} - 45r_0^2\ell^{*3} + 21r_0\ell^{*4} - 4\ell^{*5})\Omega^2}{6(r_0 - \ell^*)^5}$$

$$f_8 = -\frac{(10r_0^3 - 5r_0^2\ell^* + r_0\ell^{*2})\Omega^2}{(r_0 - \ell^*)^5}$$

$$f_9 = \frac{(12r_0^5 - 9r_0^4\ell^* + 10r_0^3\ell^{*2} - 5r_0^2\ell^{*3} + r_0\ell^{*4})\Omega^2}{6(r_0 - \ell^*)^5}$$

$$f_{10} = \frac{(27r_0^4\ell^* - 30r_0^3\ell^{*2} + 15r_0^2\ell^{*3} - 3r_0\ell^{*4})\Omega^2}{6(r_0 - \ell^*)^5}$$

$$f_{11} = -\frac{(4r_0^5 - 2r_0^4\ell^* + 10r_0^3\ell^{*2} - 10r_0^2\ell^{*3} + 5r_0\ell^{*4} - \ell^{*5})\Omega^2}{(r_0 - \ell^*)^5}$$

$$f_{12} = -\frac{(6r_0^3 - 4r_0^2\ell^* + r_0\ell^{*2})\Omega^2}{(r_0 - \ell^*)^4}$$

$$f_{13} = \frac{3r_0^3\Omega^2}{(r_0 - \ell^*)^4}$$

$$f_{14} = -\frac{(3r_0^5 + 3r_0^4\ell^*)\Omega^2}{(r_0 - \ell^*)^5}$$

$$f_{15} = \frac{4r_0^3\Omega^2}{(r_0 - \ell^*)^5}.$$

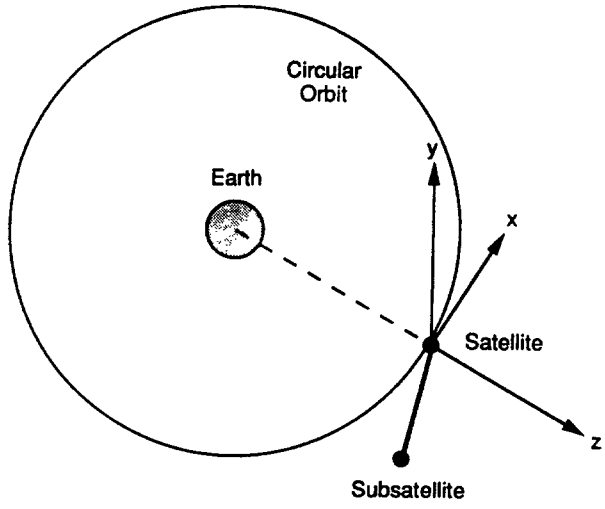

Figure 1. TSS in circular orbit.

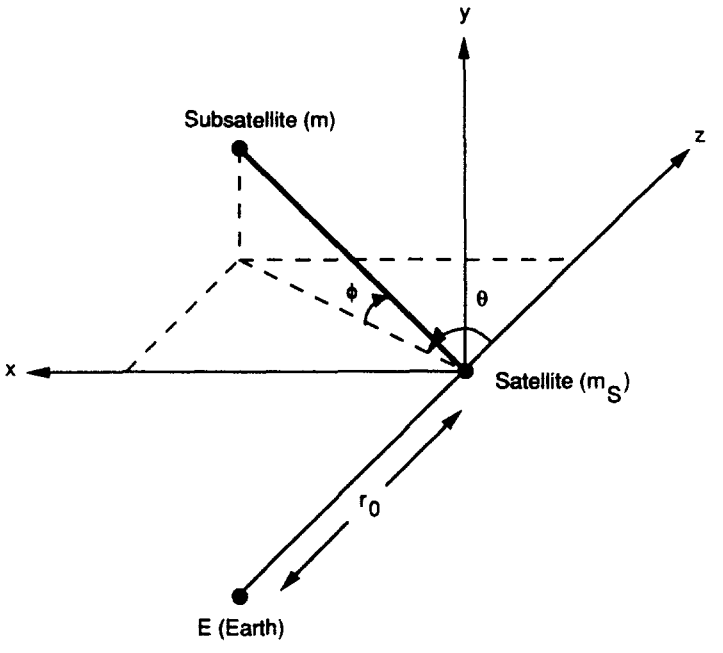

Figure 2. Rotating coordinate system.

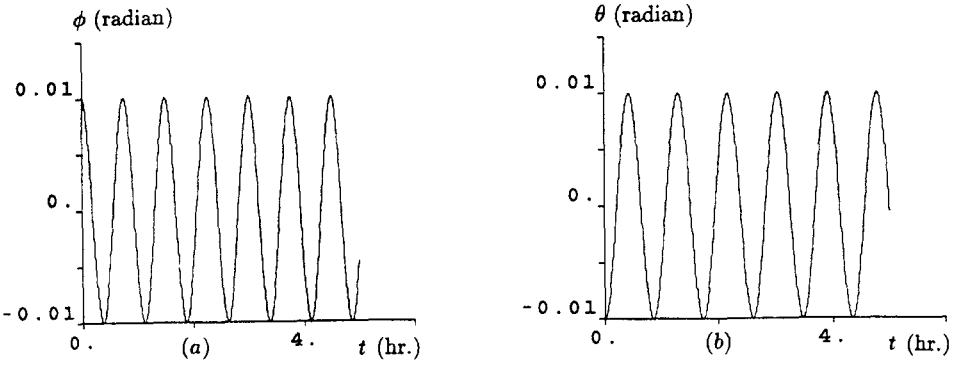

Figure 3. Simulation results for uncontrolled system.

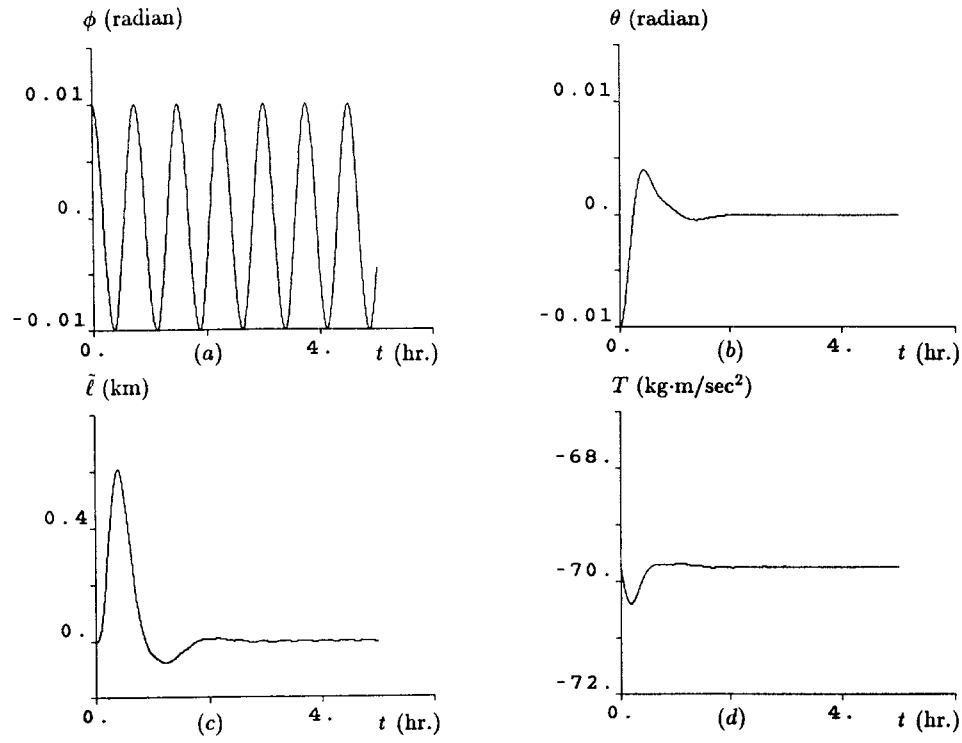

Figure 4. Simulation results for linear feedback system.

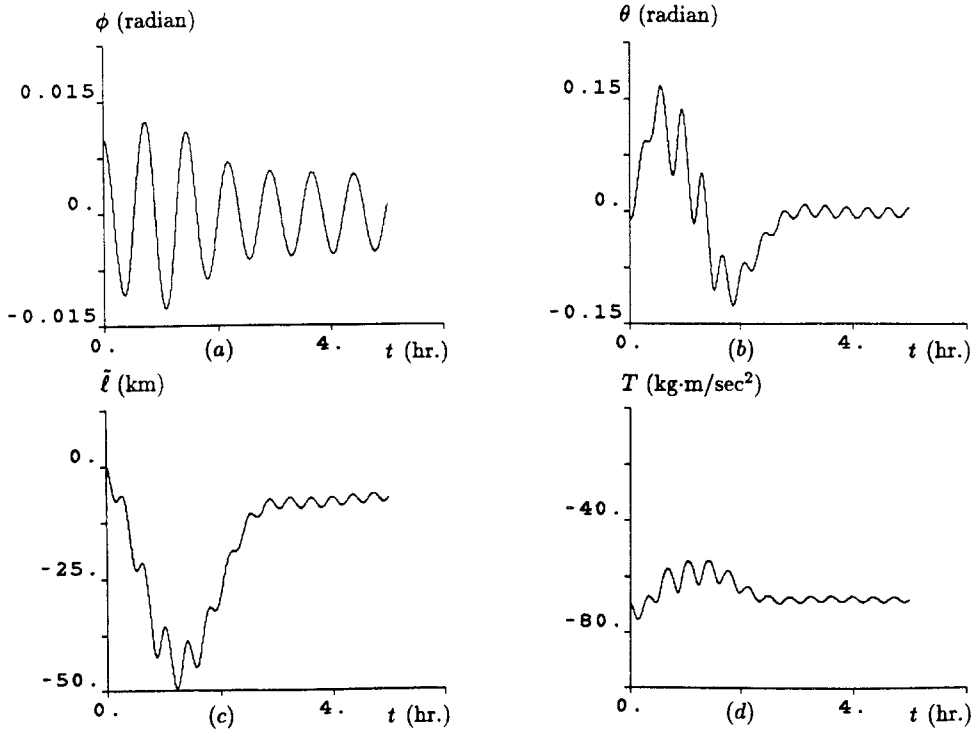

Figure 5. Simulation results for nonlinear feedback system ($q_1 = 1500$).

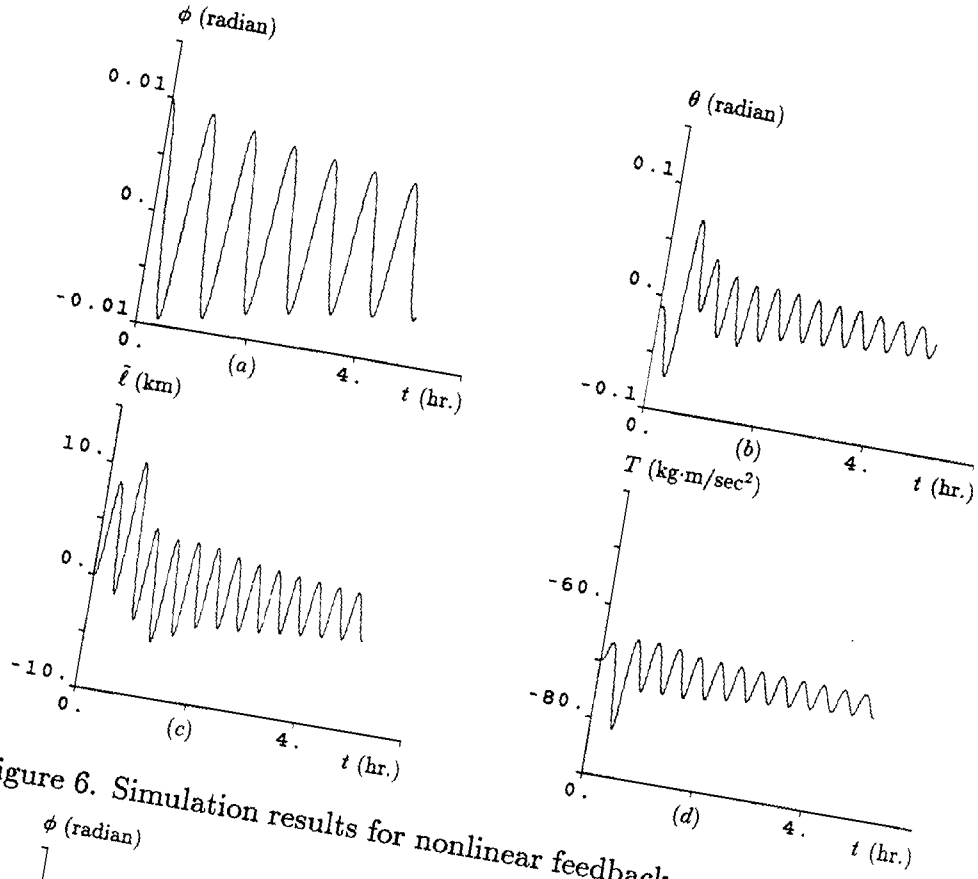

Figure 6. Simulation results for nonlinear feedback system ($q_2 = 10^6$).

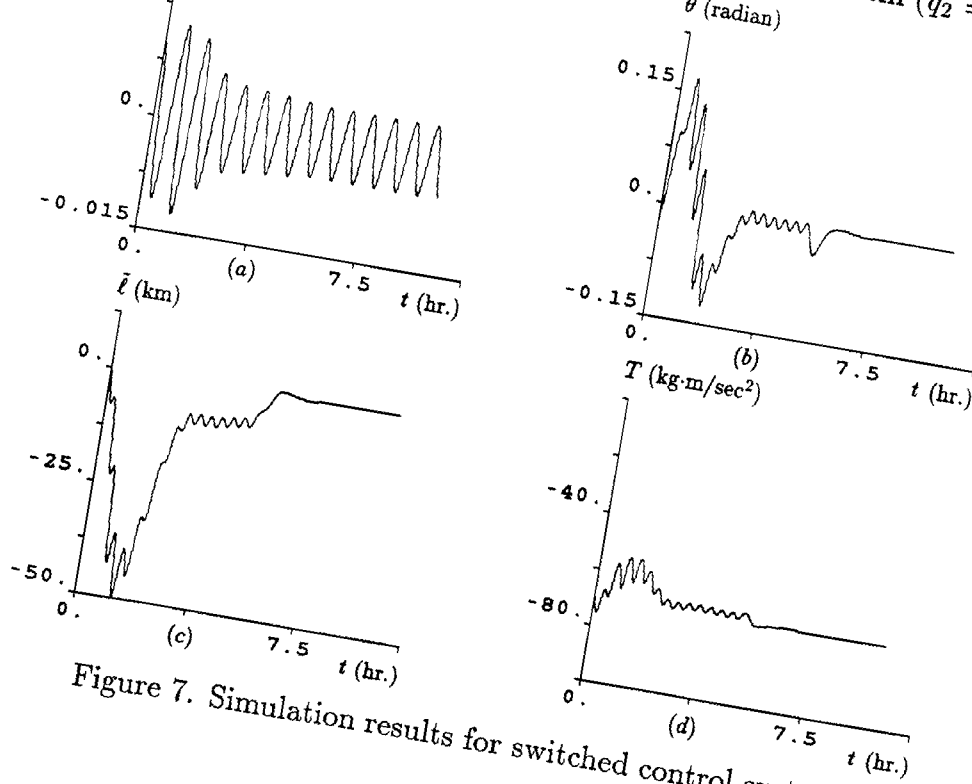

Figure 7. Simulation results for switched control system.